HHS Public Access

Author manuscript

J Cell Physiol. Author manuscript; available in PMC 2020 July 01.

Published in final edited form as:

J Cell Physiol. 2019 July ; 234(7): 10184–10195. doi:10.1002/jcp.27688.

G Protein α Subunit 14 Mediates Fibroblast Growth Factor 2-Induced Cellular Responses in Human Endothelial Cells

Qing-yun Zou[1], **Ying-jie Zhao**[1,2], **Chi Zhou**[1], **Ai-xia Liu**[1,3], **Xin-qi Zhong**[1,4], **Qin Yan**[1,5], **Yan Li**[1], **Fu-xian Yi**[1], **Ian M. Bird**[1], and **Jing Zheng**[1,6]

[1]Department of Obstetrics and Gynecology, University of Wisconsin-Madison, Madison, Wisconsin

[2]Department of Rheumatology, Qilu Hospital, Shandong University, Jinan, Shandong, China

[3]Department of Reproductive Endocrinology, Zhejiang University, Hangzhou, Zhejiang, China

[4]Department of Pediatrics, The Third Affiliated Hospital of Guangzhou Medical University, Guangzhou, Guangdong, China

[5]Department of Gynecology, Shanghai First Maternity and Infant Hospital, Tongji University School of Medicine, Shanghai, China

[6]Cardiovascular Medicine Center, Affiliated Hospital of Guangdong Medical University, Zhanjiang, Guangdong, China

Abstract

During pregnancy, a tremendous increase in fetoplacental angiogenesis is associated with elevated blood flow. Aberrant fetoplacental vascular function may lead to pregnancy complications including pre-eclampsia. Fibroblast growth factor 2 (FGF2) and vascular endothelial growth factor A (VEGFA) are crucial regulators of fetoplacental endothelial function. G protein α subunit 14 (GNA14), a member of Gαq/11 subfamily is involved in mediating hypertensive diseases and tumor vascularization. However, little is known about roles of GNA14 in mediating the FGF2- and VEGFA-induced fetoplacental endothelial function. Using human umbilical vein endothelial cells (HUVECs) cultured under physiological chronic low oxygen (3% O_2) as a cell model, we show that transfecting cells with adenovirus carrying GNA14 complementary DNA (cDNA; Ad-*GNA*14) increases ($p < 0.05$) protein expression of GNA14. GNA14 overexpression blocks ($p < 0.05$) FGF2- stimulated endothelial migration, whereas it enhances ($p < 0.05$) endothelial monolayer integrity (maximum increase of ~35% over the control at 24 hr) in response to FGF2. In contrast, GNA14 overexpression does not significantly alter VEGFA-stimulated cell migration, VEGFA-weakened cell monolayer integrity, and intracellular Ca^{++} mobilization in response to adenosine triphosphate (ATP), FGF2, and VEGFA. GNA14 overexpression does not alter either FGF2- or VEGFA-induced phosphorylation of ERK1/2. However, GNA14 overexpression time-dependently elevates ($p < 0.05$) phosphorylation of phospholipase C-β3 (PLCβ3) at S1105 in

Correspondence: Jing Zheng, PhD, Department of Obstetrics and Gynecology, University of Wisconsin-Madison, PAB1 UnityPoint Health-Meriter Hospital, 202S. Park St., Madison, WI 53715. jzheng@wisc.edu.

CONFLICTS OF INTERESTS

The authors have no conflicts of interest to disclose.

response to FGF2, but not VEGFA. These data suggest that GNA14 distinctively mediates fetoplacental endothelial cell migration and permeability in response to FGF2 and VEGFA, possibly in part by altering activation of PLCβ3 under physiological chronic low oxygen.

Keywords

angiogenesis; endothelial cells; FGF2; GNA14; VEGFA

1 | INTRODUCTION

During normal pregnancy, increased fetoplacental angiogenesis and vasodilation are associated with dramatically elevated fetoplacental blood flow, to support the increasing need for maternal and fetal exchange (Magness & Zheng, 1996). Dysregulation of fetoplacental angiogenesis may lead to adverse pregnant outcomes (Zygmunt, Herr, Münstedt, Lang, & Liang, 2003) such as pre-eclampsia (PE, a hypertensive disorder during pregnancy; Boeldt & Bird, 2017; Cerdeira & Karumanchi, 2012; Zygmunt et al., 2003). Thus, a better understanding of mechanisms underlying placental angiogenesis will help us develop strategies to control abnormal angiogenesis.

Heterotrimeric G proteins mediate many cell function, affecting diverse biological processes including cardiovascular growth and function (Pyne & Pyne, 2011). The G protein α subunit is a major signaling transducer of heterotrimeric G proteins, and is currently grouped into four subfamilies: Gα_s, G$\alpha_{i/o}$, G$\alpha_{q/11}$, and G$\alpha_{12/13}$ with a total of 18 members in humans (Syrovatkina, Alegre, Dey, & Huang, 2016; Wettschureck & Offermanns, 2005). Among these members, G protein α subunit 14 (GNA14), a member of G$\alpha_{q/11}$ subfamily, is expressed in endothelial cells of human placentas and umbilical cord vessels and its expression in human placentas is elevated by ~nine-fold during pregnancy (Zhao et al., 2014). More important, whereas GNA14 has been identified as a human hypertension-susceptibility gene (Kohara et al., 2008), its protein levels are elevated (~three-fold vs. normotensive pregnancy) in human placental tissues from patients with PE (Zhao et al., 2014) and in lung tissues from patients with pulmonary artery hypertension (PAH; Abdul-Salam et al., 2010; Lei et al., 2014). To date, it is unknown if there are increases in endothelial GNA14 protein expression in PE placental and PAH lung (Zhao et al., 2014; Zou et al., 2018). However, these data suggest that GNA14 overexpression is involved in human hypertensive disorders and other vascular diseases (e.g., congenital and sporadic vascular tumor, Lim et al., 2016), which are often associated with impaired endothelial function.

Fibroblast growth factor 2 (FGF2) and vascular endothelial growth factor A (VEGFA) are key regulators of fetoplacental endothelial function (Wang & Zheng, 2012). FGF2- and VEGFA-induced cellular function are mediated primarily via activation of their receptor tyrosine kinases (RTKs; Ferrara, Gerber, & LeCouter, 2003; Klein, Roghani, & Rifkin, 1997; Wang & Zheng, 2012). These RTKs in turn induce a vast array of signaling pathways including mitogen-activated protein kinase 3/1 (ERK1/2) (Wang & Zheng, 2012), leading to subsequent cell responses (Ferrara et al., 2003; Podar & Anderson, 2008; Turner & Grose, 2010; Wang & Zheng, 2012).

Coexpression of GNAq and 11, another two members of $G\alpha_{q/11}$ subfamily, has been reported to be important in mediating FGF2 and/or VEGFA-induced endothelial responses including endothelial proliferation, migration, and intracellular Ca^{++} mobilization (Mukhopadhyay & Zeng, 2002; Sivaraj et al., 2015; Zeng, Zhao, & Mukhopadhyay, 2002, Zeng, Zhao, Yang, Datta, & Mukhopadhyay, 2003). Recently, we have also demonstrated that GNA11 alone mediates FGF2- and VEGFA-induced cell responses in human umbilical cord endothelial cells (HUVECs; Zou et al., 2018). To date, although GNA11 has ~70% amino acid sequence identity with GNA14 in humans (Hubbard & Hepler, 2006), nothing is known about the roles of GNA14 in mediating fetoplacental endothelial function. However, as a somatic constitutively active mutation of GNA14 promotes excessive vascular growth in vascular tumors, and expression of this mutation in primary HUVECs maintains cell viability in association with increased activation of ERK1/2 under a serum-free state (Lim et al., 2016), GNA14 dysregulation may contribute to fetoplacental endothelial dysfunction during the PE.

Phospholipase C β subfamily (PLCβ) is the major downstream signaling molecule of the Gαq/11 subfamily (Offermanns, 1999; Rhee, 2001). Among all four members of PLCβ subfamily (PLCβ1–4), PLCβ3 has the highest affinity to $G\alpha_{q/11}$ subfamily members (PLCβ4 and β3 ≥ PLCβ1 ≫ PLCβ2; Offermanns, 1999). PLCβ3 may differentially mediate VEGFA-induced endothelial responses, as evidenced by the observation that knockdown of PLCβ3 inhibits VEGFA-stimulated cell migration, whereas it enhances VEGFA-stimulated endothelial cell proliferation (Bhattacharya et al., 2009). Currently, it is unclear exactly how PLCβ3 is activated; however, phosphorylation of PLCβ3 at different sites such as serine 537 (S537) or 1105 (S1105) is thought to be one of the major mechanisms in regulating PLCβ3 activity (Bhattacharya et al., 2009; Xia, Bao, Yue, Sanborn, & Liu, 2001; Yue & Sanborn, 2001; Yue, Dodge, Weber, & Sanborn, 1998). Specifically, phosphorylation of PLCβ3 S1105 inhibits PLCβ3 activity in COSM6 and COS-7 cells (Xia et al., 2001; Yue et al., 1998), but the function of S537 phosphorylation remains ambiguous (Yue &Sanborn, 2001). Our recent study has also shown that elevated phosphorylation of PLCβ3S537 is associated with VEGFA-stimulated cellular responses; however, over-phosphorylation of PLCβ3 S537 is accompanied with decreased FGF2- and VEGFA-stimulated cell migration induced by GNA11 knockdown in HUVECs (Zou et al., 2018). These data suggest that phosphorylation of PLCβ3 might differentially mediate PLCβ3 S537 activity, leading to distinct cell responses.

In the current study, we tested the hypothesis that GNA14 overexpression disrupts FGF2- and VEGFA-induced fetoplacental endothelial function via altering phosphorylation of ERK1/2 and PLCβ3 in HUVECs, which were constantly cultured under physiological low oxygen (3% O_2). This low oxygen is comparable with the oxygen levels in vivo since fetoplacental endothelial cells reside under 3–8% O_2 throughout pregnancy (Jauniaux, Watson, & Burton, 2001) and HUVECs at the end of gestation are exposed to 3.7% O_2 (range 2.3–5.1%; Meschia, 2013). These oxygen levels are critical to normal endothelial function (Mayhew, 2003; Zamudio, 2007).

2 | MATERIALS AND METHODS

2.1 | Ethical approval

The protocol for collecting umbilical cords and studies conducted were approved by the Institutional Review Board of UnityPoint Meriter Hospital (Madison, WI), and the Health Sciences Institutional Review Boards of the University of Wisconsin–Madison (Protocol number 2004–006). The patients gave written, informed consent before participating.

2.2 | Isolation and culture of primary HUVECs

HUVECs were isolated from umbilical cord vein of normal pregnancy using a standard collagenase enzyme-based protocol and cultured as previously described (Jiang et al., 2013a, 2013b, 2014; Zhou et al., 2017; Zou et al., 2018). After isolation, cells were cultured in endothelial culture medium (ECM; catalog number 1001 Sciencell, Carlsbad, CA). ECM consisted of ECM basal media (ECM-b; catalog number 1001-b, Sciencell) supplemented with 5% fetal bovine serum (FBS), 1% penicillin/streptomycin (p/s), 1% amphotericin B (AB; catalog number 15290018, Thermo Fisher Scientific, Waltham, MA), and 1% endothelial cell growth supplement (ECGS) under a physiological low-oxygen condition (37°C, 5% CO_2, 3% O_2, ~92% N_2; Jiang et al., 2013b, 2013a, 2014; Zou et al., 2018). Endothelial cell phenotypes were verified as described (Jiang et al., 2013a, 2013b, 2014). Only the cell preparations with ≥ 96% of cells exhibiting CD31 positivity and uptake of DiI-Ac-LDL, and being capable of forming capillary-like tube structures were used in this study. After verification, cells were pooled from five individual cell preparations, and cells at passage 4 were used in this study (Zou et al., 2018).

All media used for cell culture and experiments were pre-purged with N_2 and equilibrated in a hypoxia incubator adjusted to physiological low-oxygen condition before use. Dissolved O_2 in medium was monitored using a meter measuring dissolved oxygen. All experiments were conducted either in a hypoxia incubator adjusted to physiological low-oxygen condition or a 3% O_2 heated oxygen-controlled glovebox (Coy Laboratory Products, Grass Lake, MI).

2.3 | Adenoviral transfection

To study the roles of GNA14 in FGF2- and VEGFA-induced cell responses in HUVECs, and to mimic its placental expression in PE, GNA14 was overexpressed using commercially available adeno-viruses carrying *GNA14* and green fluorescent protein (GFP, as reporter; Ad-*GNA14*; Vector Biolabs, Malvern, PA). Adenoviruses carrying GFP reporter alone (Ad-*GFP*) were used as a vector control (Ren et al., 2014). Amplification and transduction of adenovirus were performed as described (Jiang et al., 2014; Liao et al., 2009; Zou et al., 2018). The specificity of Ad-*GNA14* has been verified as described (Zou et al., 2018).

After the verification of specificity of Ad-*GNA14*, HUVECs at 50–60% confluence were transfected by Ad-*GNA14* or Ad-*GFP* for 3 days, and cell lysates were subjected to Western blot analysis to confirm GNA14 overexpression. Additional cells were transfected for 2 days and serum starved, followed by function assays as described below.

2.4 | GNA14 siRNA transfection

To further dissect roles of GNA14 in FGF2- and VEGFA-induced cell responses in HUVECs, GNA14 small interfering RNA (siRNA) transfection in native HUVECs without Ad-*GNA14* transfection was performed as described (Jiang et al., 2014; Li, Wang, Zou, Magness, & Zheng, 2015; Wang, Song, Chen, & Zheng, 2008; Zou et al., 2018). A pool of four siRNAs specifically targeting human GNA14 (catalog number L-008561-00-0005; GenBank number NM_004297.3; Dhar-macon, Lafayette, CO) and a pool of four scrambled siRNAs (ssiRNA; catalog number D-001810-10-05) were purchased (Dharmacon). The GNA14 siRNA and ssiRNA were premixed with Lipofectamine RNAiMAX transfection reagent (vehicle; catalog number 13778030, Invitrogen, Carlsbad, CA) at room temperature. Subconfluent cells were cultured in antibiotic and serum-free media (ECMb) containing GNA14 siRNA or ssiRNA (20 nM). After 4 hr of transfection, an equal amount of 2x ECM containing 10% FBS, 2% p/s, 2% AB 2%, and ECGS was added. Cells were cultured for 2, 3, and 4 days and lysed. Lysate proteins (20–30 μg) were subjected to Western blot. Additional cells were transfected with a second dose of GNA14 siRNA at 4 days after the first transfection, and cultured for an additional 2, 3, or 4 days before cells were harvested for Western blot.

2.5 | Cell migration

Cell migration was assayed using a transwell system (Corning, Corning, NY) as described (Jiang et al., 2014; Li et al., 2015; Zou et al., 2018). After 2 days of transfection with Ad-*GFP* or Ad-*GNA14*, cells were serum starved for 24 hr and seeded into inserts at 30,000 cells/insert. FGF2 or VEGFA was added to bottom chambers (final concentration: 100 ng/ml; catalog number 10014-HNAE and 80006-RNAB, respectively, Sino Biologic Inc, China). After 16 hr of culture, calcein AM (catalog number C3100MP, Invitrogen) was added to bottom chambers (0.2 μg/ml). Five pictures were taken randomly using a Nikon TE2000U inverted microscope. Cell numbers were quantified using the Metamorph imaging analysis program (Molecular Devices, Sunnyvale, CA). ECMb supplemented with 2% heated inactivated FBS, 1% p/s, and 1% AB was used for preparing control medium and growth factor solutions.

2.6 | Cell proliferation

Cell proliferation was evaluated using the Cell Counting Kit-8 (CCK-8; catalog number CK04–05, Dojindo Molecular Technologies, Rockville, MD) according to manufacturer's instructions. Briefly, after 2 days of transfection with Ad-*GFP* or -*GNA14*, cells were inoculated into 96-well plates (5,000–8,000 cells/well) and cultured overnight. After serum starvation for 16 hr, cells were treated with control medium, FGF2 or VEGFA (100 ng/ml) for 48 hr. CCK-8 solution was added and incubated for additional 4 hr. The OD value of each well was measured by a microplate reader at 450 nm (Bio-Tek, Winooski, VT). ECMb supplemented with 0.2% heated inactivated FBS, 1% p/s, and 1% AB was used for preparing control medium, and growth factor solutions.

2.7 | Cell monolayer integrity

Cell monolayer integrity was examined using an electric cell–substrate impedance sensing system (ECIS ZΘ; Applied Biophysics, Troy, NY) as described before (Zhou C. et al., 2017; Zou Q. et al., 2018). After 2 days of transfection with the Ad-*GFP* or Ad-*GNA14*, cells (50,000 cells/well) were inoculated into 96W10idf ECIS array plates (Applied Biophysics) precoated with 10 nM cysteine and 0.1% gelatin. Resistance of each well was monitored at 4,000 Hz. After resistance reached a plateau (indicating 100% confluence), cells were serum starved for 3–4 hr in ECMb containing 1% p/s and 1% AB. FGF2 or VEGFA was added (100 ng/ml) and the resistance was monitored for up to 24 hr as an indicator of cell monolayer integrity.

2.8 | $[Ca^{++}]_i$ imaging

Intracellular calcium concentration ($[Ca^{++}]_i$) was monitored as described (Boeldt et al., 2017; Krupp et al., 2013). HUVECs at passage 4 (300,000 cells) were plated into 35 mm glass-bottom dishes and cultured overnight. After transfection with Ad-*GNA14* or Ad-*GFP* for 3 days, HUVECs were incubated in 10 μM Fura-2 AM with 0.05% pluronic acid F127 (Life Technologies, Carlsbad, CA) dissolved in 1 ml ECM for an hour in a hypoxic incubator. Cells were incubated in Krebs buffer (125 mM NaCl, 5 mM KCl, 1 mM $MgSO_4$, 1 mM KH_2PO_4, 6 mM glucose, 2 mM $CaCl_2$, 25 mM HEPES, pH 7.4) for 30 min for ester hydrolysis. Fura-2 loading was verified by viewing 380-nm UV excitation on a Nikon inverted microscope and 80–90 cells were selected for imaging. An initial 5 min basal level recording was performed before subsequent addition of 100 μM ATP, a positive control for endothelial $[Ca^{++}]_i$ response mediated via G-protein coupled heptahelical receptors, FGF2 (100 ng/ml) or VEGFA (100 ng/ml; catalog number 293-VE-010, R&D Systems, Minneapolis, MN). In preliminary studies, similar $[Ca^{++}]_i$ responses were also observed in cells treated with VEGFA from Abgent (catalog number 80006-RNAB; data not shown). After treatment with ATP, FGF2, and VEGFA, $[Ca^{++}]_i$ was monitored for up to 30 min. $[Ca^{++}]_i$ for each cell was calculated in real-time against an established ratiometric standard curve using InCyt Im2 software (Intracellular Imaging, Cincinnati, OH). Changes in $[Ca^{++}]_i$ were expressed as fold of the mean value of the last minute of the basal level. The area under curve for VEGFA-induced changes in $[Ca^{++}]_i$ was calculated using SigmaPlot software (Jandel Co., San Rafael, CA).

2.9 | Western blot analysis

Western blot analysis was conducted as described (Jiang et al., 2013a, 2013b, Li et al., 2017, 2015; Zou et al., 2018). Cells were disrupted in lysis buffer (50 mM HEPES, 0.1 M NaCl, 10 mM ethylenediaminetetraacetic acid (EDTA), 4 mM sodium pyrophosphate, 10 mM sodium fluoride, 2 mM sodium orthovanadate [pH 7.5], 1 mM phenylmethylsulfonylfluoride, 1% Triton X-100, 5 μg/ml leupeptin, and 5 μg/ml aprotinin) and centrifuged. Protein samples (20–30 μg/sample) were separated on 10% sodium dodecyl sulfate-polyacrylamide gel electrophoresis (SDS-PAGE) gels, and electrically transferred to polyvinylidene difluoride membranes. Membranes were probed by primary antibodies (Table 1). Proteins were visualized by enhanced chemiluminescence (ECL) or ECL2

(Thermo Fisher Scientific). Signals were recorded by Epson Perfection 4990 Photo Scanner (Long Beach, CA). Data were analyzed using the NIH Image J software.

2.10 | Statistics

Data were analyzed using one-way analysis of variance (ANOVA) or Student's *t*-test (SigmaPlot software). When an F-test was significant, data were analyzed using the Student-Newman–Keuls (SNK) Method for pairwise multiple comparisons. Results was considered statistically significant when $p < 0.05$.

3 | RESULTS

3.1 | Ad-*GNA14* increases protein levels of GNA14

After 3 days of transfection, Ad-*GNA14* ($p < 0.05$) dose-dependently elevated protein levels of GNA14 and GNA11 (Figure 1a). Specifically, Ad-*GNA14* at 5 multiplicity of infection (MOI) significantly increased ($p < 0.05$) GNA14 (~5 fold of control), but not GNA11, whereas Ad-*GNA14* at 10 and 20 MOI elevated ($p < 0.05$) both GNA14 (~7.8 and ~18.5 fold, respectively) and GNA11 (~2.5 and ~7.4 fold, respectively). Ad-*GFP* had no significant effects on either GNA14 or GNA11 protein levels in HUVECs as previously reported (Zou et al., 2018).

Since Ad-*GNA14* at 5 MOI significantly ($p < 0.05$) elevated only GNA14, but not GNA11 protein levels (Figure 1a), which was comparable to the ~2.5–2.9 fold increase in GNA14 protein observed in human placentas from PE as compared with normotensive pregnancy (Zhao et al., 2014), Ad-*GNA14* at 5 MOI was used in all of the following experiments.

We have also attempted to further confirm the role of GNA14 in HUVECs using the siRNA method. We observed that neither a single nor double dosing of GNA14 siRNAs at 20 nM significantly altered GNA14 protein levels (Figure 1b; quantitative data not shown). We had also transfected cells with 40 and 100 nM of GNA14 siRNA for up to 4 days. However, neither of these two doses of GNA14 siRNA significantly changed GNA14 protein levels (data not shown). As we were unable to suppress GNA14 protein expression using GNA14 siRNA in HUVECs, no further loss of function assays were performed.

3.2 | Ad-*GNA14* alters cell migration and monolayer integrity in response to FGF2, but not VEGFA

Compared with the control medium (ECM-b), FGF2 and VEGFA significantly ($p < 0.05$) stimulated cell migration by ~3.1 and ~4.8 fold, respectively (Figure 2a). However, Ad-*GNA14*, but not Ad-*GFP*, blocked ($p < 0.05$) FGF2-induced cell migration, whereas it did not significantly affect VEGFA-stimulated cell migration.

Compared with the control, FGF2 and VEGFA ($p < 0.05$) stimulated cell proliferation in the 0 MOI group (~2.2 and ~1.8 fold, respectively) and in the Ad-*GFP* group (~1.9 and ~1.8 folds, respectively; Figure 2b). However, Ad-*GFP* alone also significantly ($p < 0.05$) stimulated cell proliferation (~1.6 fold) in the 0 MOI group (Figure 2b), suggesting an off-target stimulatory effect of Ad-*GFP*. Thus, as Ad-*GNA14* also contains *GFP*, we cannot exclude the possibility that *GFP* would partially contribute to FGF2- and VEGFA-stimulated

cell proliferation in the Ad-*GNA14* group. Nevertheless, Ad-*GNA14* completely inhibited ($p < 0.05$) FGF2/GFP- and VEGFA/GFP-stimulated cell proliferation (Figure 2b).

Compared with the control, FGF2 did not significantly affect cell monolayer integrity, whereas VEGFA decreased ($p < 0.05$) the cell resistance or decreased cell monolayer integrity by ~40%, starting at~4 hr (Figure 2c,d) in the 0 MOI and Ad-GFP groups. Interestingly, Ad-*GNA14* time-dependently elevated ($p < 0.05$) the cell resistance or elevated monolayer integrity in response to FGF2, but not VEGFA (Figure 2c,d) indicating decreases in cell permeability. This elevation in cell resistance began at ~8 hr of the FGF2 treatment (~17%) and was maintained for up to 24 hr (~35% at 24 hr).

3.3 | Ad-*GNA14* does not change $[Ca^{++}]_i$ in response to ATP, FGF2, and VEGFA

We also examined effects of Ad-GNA14 on $[Ca^{++}]_i$ mobilization in response to ATP, FGF2, or VEGFA. We observed that ATP (Figure 3a,b) VEGFA (Figure 3e,f), but not FGF2 (Figure 3c,d) increased ($p < 0.05$) $[Ca^{++}]_i$. In the 0 MOI group, the VEGFA-induced $[Ca^{++}]_i$ peak was delayed for 2–3 min compared with ATP treatments, and the magnitude of this peak appeared to be slightly lower than that induced by ATP (~2 vs. ~3 fold, respectively). However, compared with the 0 MOI group, Ad-*GFP* and -*GNA14* did not change VEGFA-induced $[Ca^{++}]_i$ peak (Figure 3). The area under curve between 0 and 10 min of the VEGFA treatment was also calculated; but no significant differences ($p = 0.205$) were found between 0 MOI (1.0 ± 0.09 of fold of 0 MOI), Ad-*GFP* (1.3 ± 0.14), and Ad-*GNA14* (1.3 ± 0.09) groups.

The proportions of cells responding to ATP (89.7 ± 3.05%,85.9 ± 4.01%, and 89.9 ± 3.32%, respectively) or VEGFA(65.7 ± 10.54%, 72.9 ± 7.09%, and 73.6 ± 9.13%, respectively) were also similar among the 0 MOI, Ad-*GFP*, and Ad-*GNA14* groups. No cell responded to FGF2.

3.4 | Ad-*GNA14* does not affect FGF2-induced phosphorylation of ERK1/2

Both FGF2 and VEGFA time-dependently increased ($p < 0.05$) phosphorylation of ERK1/2 at T202/Y204 (~16.6 and ~6.1 fold increases at 10 min versus time 0 for FGF2 and VEGFA, respectively; Figure 4). Ad-*GNA14* did not alter FGF2-induced phosphorylation of ERK1/2 for up to 60 min (Figure 4a). Ad-GNA14 significantly increased ($p < 0.05$) VEGFA-induced phosphorylation of ERK1/2 only at 30 min (~3.3 folds) but not at other time points studies (Figure 4b).

3.5 | Ad-*GNA14* increases phosphorylation of PLCβ3 S1105 in response to FGF2, but not VEGFA

In the 0 MOI group, compared with the time 0 control, FGF2 did not induce phosphorylation of PLCβ3 S537 and S1105 for up to 60 min (Figure 5a), whereas VEGFA rapidly (≤5 min) increased ($p < 0.05$) phosphorylation of PLCβ3 S537 (~14.8 fold at 5 min), but not S1105 (Figure 5b). This VEGFA-increased phosphorylation of PLCβ3 S537 was maintained at relatively high levels for up to 60 min (Figure 5b).

Ad-*GNA14* rapidly (≤ 5 min) elevated phosphorylation of PLCβ3 S537 (~ 3.4 and 6.2 folds over Ad-*GFP* at 5 and 20 min, respectively; $p < 0.05$) in response to FGF2 in a time-dependent fashion (Figure 4b). However, Ad-*GNA14* did not alter the phosphorylation patterns of PLCβ3 either at S1105 in response to FGF2, or at S537 and S1105 in response to VEGFA.

4 | DISCUSSION

In the current study, we demonstrate that under physiological low oxygen, GNA14 overexpression significantly inhibits endothelial migration and permeability in response to FGF2, but not VEGFA. This inhibition is associated with elevated phosphorylation of PLCβ3 S1105. These results indicate that GNA14 differentially regulates FGF2- and VEGFA-induced fetoplacental endothelial responses. These findings also suggest that GNA14 overexpression might impair FGF2-regulated endothelial function, perhaps contributing to fetoplacental endothelial dysfunction in PE.

We also show that overexpression of wild type GNA14 in primary HUVECs alters cell migration, monolayer integrity, and PLCβ3 phosphorylation in response to FGF2, but not VEGFA. In addition, GNA14 overexpression abolishes both FGF2/GFP- and VEGFA/GFP-stimulated cell proliferation, but does not alter $[Ca^{++}]_i$ in response ATP, FGF2, or VEGFA. To our knowledge, this is the first report of differential roles of GNA14 in mediating FGF2- and VEGFA-induced fetoplacental endothelial function. Interestingly, whereas GNA11 mediates both FGF2- and VEGFA-stimulated cell migration, but not proliferation and permeability in HUVECs (Zou et al., 2018), GNA14 exclusively acts on FGF2-, but not VEGFA-regulated cell responses examined in the current study. Thus, these data support the concept that GNA11 and GNA14 have common and differential roles in mediating FGF2- and VEGFA-induced cellular response as previously suggested (Hubbard & Hepler, 2006; Nakamura, Nukada, Imai, & Sugiyama, 1996). It is unknown if FGF2 treatment regulates expression of GNA14. However, in the Ad-*GNA14* group, FGF2 induced rapid cellular migration (16 hr), monolayer integrity (staring at 8 hr), and increases in PLCβ3 phosphorylation (within 5 min). Thus, this acute FGF2 treatment is unlikely to affect GNA14 protein expression.

It is noteworthy that although we have verified the specificity of Ad-*GNA14* (Zou et al., 2018), Ad-*GNA14* at high doses (10 and 20 MOI) elevates GNA11 protein levels in HUVECs. It is unclear if Ad-*GNA14* also alters expression of other $G\alpha_{q/11}$ subfamily members such as GNAq as they all are high identical in amino acid sequences. However, at a relatively low MOI (e.g., 5 MOI), Ad-*GNA14* is unlikely to increase such nonspecific expression as we observed for GNA11 in the current study. Thus, together with our recent report showing that Ad-*GNA11* increases GNA14 protein levels (Zou et al., 2018), it is possible that there exists yet to be identified mechanisms by which expression of members of Gαq/11 subfamily regulated in a reciprocal fashion.

We have attempted to further define the role of GNA14 in HUVECs using siRNA to knockdown GNA14. However, no dosage schedule of pooled GNA14 siRNA examined suppresses GNA14 protein expression (Figure 1b), despite the evidence from real-time

quantitative polymerase chain reaction (RT-qPCR) analysis showing that after 2 days of transfection, GNA14 siRNA at 20 nM decreases GNA14 messenger RNA (mRNA) levels by ~50% (data not shown). We have also tested single GNA14 siRNA from two additional vendors (Integrated DNA Technologies, Skokie, IL and Santa Cruz Biotechnology, Dallas, Texas); but these GNA14 siRNAs also failed significantly knockdown GNA14 protein (data not shown). These data suggest that GNA14 siRNAs used in the current study are insufficient to suppress GNA14 protein expression in HUVECs. Alternatively, another explanation could be that GNA14 protein expression is uniquely regulated at the posttranslational level in HUVECs as such suppression of GNA14 mRNA expression might decrease degradation of GNA14 protein in HUVECs.

Interestingly, we have observed an off-target, stimulatory effect of Ad-*GFP*, specifically on cell proliferation. This finding raises a caution against using Ad-*GFP* as a control in future studies. However, this observation is not surprising since Ad-*GFP* alone stimulates cell proliferation, migration, and tube formation in human lung micro-vascular endothelial cells under a serum-free condition via activation of focal adhesion kinase (Kornberg & Grant, 2007). In addition, compared with Ad-*GFP*, neither FGF2 nor VEGFA further promotes cell proliferation, indicating no synergistic effects on cell proliferation. Thus, we cannot draw a conclusion about the specific role of GNA14 overexpression in FGF2- and VEGFA-stimulated cell proliferation. Nonetheless, it is noteworthy that even though Ad-GFP exhibits the off-target effect on cell proliferation, GNA14 over-expression blocks cell proliferation stimulated by FGF2/Ad-*GFP* and VEGFA/Ad-*GFP*, supporting its antiproliferative activity.

The current finding that in Ad-*GFP*-transfected cells, both FGF2 and VEGFA stimulate ERK1/2 phosphorylation in HUVECs is consistent with our previous reports (Jiang et al., 2013a; Wang & Zheng, 2012). However, in contrast to our hypothesis, GNA14 overexpression does not change the overall phosphorylation pattern of ERK1/2 at T202/Y204 induced by FGF2 and VEGFA. Thus, similar to GNA11 (Zou et al., 2018), GNA14 may not play a major role in mediating FGF2- and VEGFA-induced activation of ERK1/2 under physiological chronic low O_2. This prompts us to ask what other signaling molecules might participate in GNA14-mediated FGF2′s action in HUVECs. One potential signaling molecule is PLCβ3, since it is a major downstream target of members of the G$\alpha_{q/11}$ subfamily and a key mediator of many VEGFA's actions in endothelial cells (e.g., migration and proliferation; Hubbard & Hepler, 2006; Mukhopadhyay & Zeng, 2002; Offermanns, 1999; Sivaraj et al., 2015; Zeng et al., 2002, 2003; Zou et al., 2018).

Indeed, we observe that VEGFA induces phosphorylation of PLCβ3 S537, though FGF2 does not induce phosphorylation of PLCβ3 S537 and 1105 in the Ad-*GFP* group. These observations are agreement with our recent report (Zou et al., 2018), further confirming our suggestion that phosphorylation levels of PLCβ3 537 and 1105 is involved in VEGFA-, but not FGF2-induced cell function under basal physiological conditions (Zou et al., 2018). More important, GNA14 overexpression elevates phosphorylation of PLCβ3 S1105 in response to FGF2 in parallel to decreased cell migration, increased monolayer integrity, and unaltered ERK1/2 activation. Thus, it is reasonable to propose that GNA14 serves as a positive mediator of phosphorylation of PLCβ3 S1105 in response to FGF2. In addition, it indicates that similar to GNA11, GNA14 also does not mediate ERK1/2 activation in

HUVECs. Together with the previous reports that phosphorylation of PLCβ3 S1105 inhibits PLCβ3 activity (Xia et al., 2001; Yue et al., 1998; Yue, Ku, Liu, Simon, & Sanborn, 2000), our current observations suggest that GNA14 overexpression-elevated phosphorylation of PLCβ3 S1105 may attenuate activity of PLCβ3, partially contributing to the abolition of FGF2-stimulated cell migration and FGF2-enhanced monolayer integrity.

In contrast to the previous report that VEGFA induces phosphorylation of both PLCβ3 S537 and 1105 (Bhattacharya et al., 2009) in HUVECs, we only see phosphorylation of PLCβ3 S537, but not S1105, in response to VEGFA. It is unclear whether this discrepancy is due to the different oxygen levels used to culture cells (3% vs. presumably ~21% O_2). Nonetheless, Ad-*GNA14* fails to affect phosphorylation of PLCβ3 S537 and S1105 in response to VEGFA. These data indicate that although VEGFA-induced phosphorylation of PLCβ3 S537 may critically mediate VEGFA-induced cell function, GNA14 does not mediate such phosphorylation. Instead, GNA11, another member of G$\alpha_{q/11}$ subfamily may be a key mediator for such phosphorylation in response to VEGFA as we recently suggest (Zou et al., 2018).

Unlike GNAq and GNA11 which regulate VEGFA-stimulated $[Ca^{++}]_i$ mobilization in HUVECs (Mukhopadhyay & Zeng, 2002; Zeng et al., 2003), GNA14 overexpression does not alter VEGFA-induced $[Ca^{++}]_i$ responses, suggesting that GNA14 may not participate in the VEGFA-PLCβ3-IP3-Ca^{++} signaling pathway in HUVECs.

To date, the mechanism controlling phosphorylation of PLCβ3 S537 and S1105 is undefined in HUVECs. However, the constitutively active form of calcium/calmodulin-dependent protein kinase II induces phosphorylation of PLCβ3 S537 in COSM6 cells (Yue & Sanborn, 2001). Protein kinase A, C, and G can also phosphorylate PLCβ3 S1105 in COSM6 and COS-7 cells, inhibiting PLC activity (Xia et al., 2001; Yue et al., 1998, 2000). Thus, these protein kinases may be involved in phosphorylation of PLCβ3 S537 and S1105 in response to FGF2 and VEGFA in HUVECs. In addition, our finding that the $[Ca^{++}]_i$ response to VEGFA is delayed by a few minutes while that to ATP (a stimulant of heptahelical receptors coupled to PLCβ3) is immediate further suggests that PLCβ3 is not the central player in mediating VEGFA-induced changes in $[Ca^{++}]$i and that role is fulfilled by PLCγ. It is more likely that PLCβ3 is a player in further downstream cell signaling such as the small G protein CDC42 as described by Bhattacharya et al. (2009).

The exact interactions between the RTK cascades and GNA14 are unclear in HUVECs. Based on the data from the present and previous studies (Jiang et al., 2013a; Wang & Zheng, 2012), we would like to hypothesize that GNA14 differentially mediates phosphorylation of PLCβ3 S537 and S1105 via distinctive activation of RTK downstream signals in response to FGF2 and VEGFA under physiological chronic low oxygen as described in Figure 6. Further studies are needed to define the RTK/GNA14/PLCβ3 pathway and the role of PLCβ3 S1105 and/or S537 phosphorylation in regulating the activity of PLCβ3 in response to FGF2 and VEGFA. This is important as GNA14 and phosphorylation of PLCβ3 at different sites could be potential targets for therapeutic intervention for endothelial dysfunction.

In conclusion, our results indicate differential mediation of GNA14 in FGF2- and VEGFA-induced fetoplacental endothelial function in association with distinct phosphorylation of PLCβ3. Such findings suggest GNA14 overexpression in endothelial cells might impair endothelial function, leading to hypertension-related diseases (e.g., hypertension, PAH, and PE). Thus, our data demonstrate a unique crosstalk between GNA14 and PLCβ3, and reveal a novel signaling mechanism of FGF2 in endothelial cells.

ACKNOWLEDGMENT

We thank Laura H. Hogan, Ph.D., a Science Writer/Newsletter Editor from Institute for Clinical and Translational Research, University of Wisconsin School of Medicine and Public Health, for critically reading and editing this manuscript. We also appreciate Derek S. Boeldt, Ph.D., Assistant Professor of Ob/Gyn Dept., University of Wisconsin School of Medicine and Public Health, for his inputs in $[Ca^{++}]_i$ imaging analysis.

This study was supported in part by National Institutes of Health grant PO1 HD38843 to JZ and IMB. The project was also supported by the Clinical and Translational Science Award program, through the NIH National Center for Advancing Translational Sciences, grant UL1TR002373. The content is solely the responsibility of the authors and does not necessarily represent the official views of the NIH. This study is in partial fulfillment for a PhD degree (Q-Y Z) in the Endocrinology and Reproductive Physiology Training Program (www.erp.wisc.edu).

Funding information

Clinical and Translational Science Award program, NIH National Center for Advancing Translational Sciences, Grant/Award Number: UL1TR002373; National Institutes of Health, Grant/Award Number: PO1 HD38843

REFERENCES

Abdul-Salam VB, Wharton J, Cupitt J, Berryman M, Edwards RJ, & Wilkins MR (2010). Proteomic analysis of lung tissues from patients with pulmonary arterial hypertension. Circulation, 122(20), 2058–2067. 10.1161/CIRCULATIONAHA.110.972745 [PubMed: 21041689]

Bhattacharya R, Kwon J, Li X, Wang E, Patra S, Bida JP, … Mukhopadhyay D (2009). Distinct role of PLCβ3 in VEGF-mediated directional migration and vascular sprouting. Journal of Cell Science, 122(7), 1025–1034. 10.1242/jcs.041913 [PubMed: 19295129]

Boeldt DS, & Bird IM (2017). Vascular adaptation in pregnancy and endothelial dysfunction in preeclampsia. Journal of Endocrinology, 232(1), R27–R44. 10.1530/JOE-16-0340 [PubMed: 27729465]

Boeldt DS, Krupp J, Yi F-X, Khurshid N, Shah DM, & Bird IM (2017). Positive versus negative effects of VEGF 165 on Ca^{2+} signaling and NO production in human endothelial cells. American Journal of Physiology - Heart and Circulatory Physiology, 312(1), H173–H181. 10.1152/ajpheart.00924.2015 [PubMed: 27836897]

Cerdeira AS, & Karumanchi SA (2012). Angiogenic factos in preeclampsia and related disorders. Cold Spring Harbour Persepctives in Medicine, 2(11), 239–252. 10.1101/cshperspect.a006585

Ferrara N, Gerber H-P, & LeCouter J (2003). The biology of VEGF and its receptors. Nature Medicine, 9(6), 669–676. 10.1038/nm0603-669

Hubbard KB, & Hepler JR (2006). Cell signalling diversity of the Gqα family of heterotrimeric G proteins. Cellular Signalling, 18, 135–150. 10.1016/j.cellsig.2005.08.004 [PubMed: 16182515]

Jauniaux E, Watson A, & Burton G (2001). Evaluation of respiratory gases and acid-base gradients in human fetal fluids and uteroplacental tissue between 7 and 16 weeks' gestation. American Journal of Obstetrics and Gynecology, 184(5), 998–1003. [PubMed: 11303211]

Jiang Y-Z, Li Y, Wang K, Dai C-F, Huang S-A, Chen D-B, & Zheng J (2014). Distinct roles of HIF1A in endothelial adaptations to physiological and ambient oxygen. Molecular and Cellular Endocrinology, 391(1–2), 60–67. 10.1016/j.mce.2014.04.008 [PubMed: 24796659]

Jiang Y-Z, Wang K, Li Y, Dai C-F, Wang P, Kendziorski C, & Zheng J (2013a). Enhanced cellular responses and distinct gene profiles in human fetoplacental artery endothelial cells under chronic

low oxygen. Biology of Reproduction, 89(6), 133 10.1095/biolreprod.113.110551 [PubMed: 24152727]

Jiang Y-Z, Wang K, Li Y, Dai C-F, Wang P, Kendziorski C, & Zheng J (2013b). Transcriptional and functional adaptations of human endothelial cells to physiological chronic low oxygen. Biology of Reproduction, 88(5), 114 10.1095/biolreprod.113.108225 [PubMed: 23536375]

Klein S, Roghani M, & Rifkin DB (1997). Fibroblast growth factors as angiogenesis factors: New insights into their mechanism of action In Goldberg ID, & Rosen EM (Eds.), Regulation of Angiogenesis (79, pp. 159–192). Birkhäuser Basel 10.1007/978-3-0348-9006-9_7

Kohara K, Tabara Y, Nakura J, Imai Y, Ohkubo T, Hata A, … MIKI T (2008). Identification of hypertension-susceptibility genes and pathways by a systemic multiple candidate gene approach: The millennium genome project for hypertension. Hypertension Research: Official Journal of the Japanese Society of Hypertension, 31(2), 203–212. 10.1291/hypres.31.203 [PubMed: 18360038]

Kornberg LJ, & Grant MB (2007). Adenoviruses increase endothelial cell proliferation, migration, and tube formation: Partial reversal by the focal adhesion kinase inhibitor, FRNK. Microvascular Research, 73(3), 157–162. 10.1016/j.mvr.2007.02.005 [PubMed: 17407784]

Krupp J, Boeldt DS, Yi F-X, Grummer MA, Bankowski Anaya HA, Shah DM, & Bird IM (2013). The loss of sustained Ca^{2+} signaling underlies suppressed endothelial nitric oxide production in preeclamptic pregnancies: Implications for new therapy. AJP: Heart and Circulatory Physiology, 305(7), H969–H979. 10.1152/ajpheart.00250.2013 [PubMed: 23893163]

Lei W, Chen P, Yue Y, He Y, Shui X, Li G, … Chen C (2014). Subcellular distribution patterns and elevated expression of GNA11 and GNA14 proteins in the lungs of humans with pulmonary arterial hypertension. Cell Biology International, 38(9), 1041–1049. 10.1002/cbin.10292 [PubMed: 24797109]

Li Y, Wang K, Zou Q-Y, Jiang Y-Z, Zhou C, & Zheng J (2017). ITE suppresses angiogenic responses in human artery and vein endothelial cells: Differential roles of AhR. Reproductive Toxicology, 74 10.1016/j.reprotox.2017.09.010

Li Y, Wang K, Zou QY, Magness RR, & Zheng J (2015). 2,3,7,8-Tetrachlorodibenzo-p-dioxin differentially suppresses angiogenic responses in human placental vein and artery endothelial cells. Toxicology, 336, 70–78. 10.1016/j.tox.2015.08.003 [PubMed: 26275813]

Liao W, Feng L, Zhang H, Zheng J, Moore TR, & Chen D (2009). Compartmentalizing VEGF-induced ERK2/1 signaling in placental artery endothelial cell caveolae: A paradoxical role of caveolin-1 in placental angiogenesis in vitro. Molecular Endocrinology (Baltimore, MD), 23(9), 1428–1444. 10.1210/me.2008-0475

Lim YH, Bacchiocchi A, Qiu J, Straub R, Bruckner A, Bercovitch L, …Choate KA (2016). GNA14 somatic mutation causes congenital and sporadic vascular tumors by MAPK activation. American Journal of Human Genetics, 99(2), 443–450. 10.1016/j.ajhg.2016.06.010 [PubMed: 27476652]

Magness RR, & Zheng J (1996). Circulatory changes during gestation In Gluckman PD & Heymann MA (Eds.), Scientific Basis of Pediatric and Perinatal Medicine (pp. 762–772). London: Edward Arnold Publishers.

Mayhew TM (2003). Changes in fetal capillaries during preplacental hypoxia: Growth, shape remodelling and villous capillarization in placentae from high-altitude pregnancies. Placenta, 24(2–3), 191–198. 10.1053/plac.2002.0895 [PubMed: 12566246]

Meschia G (2013). Placental respiratory gas and exchange and fetal oxygenation In Resnik R, Creasy R & Iams J (Eds.), Maternal-Fetal Medicine: Principles and Practice (7th ed., pp. 163–174). Philadelphia: Saunders.

Mukhopadhyay D, & Zeng H (2002). Involvement of G proteins in vascular permeability factor/vascular endothelial growth factor signaling. Cold Spring Harbor Symposia on Quantitative Biology, 67, 275–283. 10.1101/sqb.2002.67.275 [PubMed: 12858550]

Nakamura K, Nukada T, Imai K, & Sugiyama H (1996). Importance of N-terminal regions of G protein alpha subunits for the activation of phospholipase C in Xenopus oocytes. Journal of Biochemistry, 120(5), 996–1001. http://www.ncbi.nlm.nih.gov/pubmed/8982868 [PubMed: 8982868]

Offermanns S (1999). New insights into the in vivo function of heterotrimeric G-proteins through gene deletion studies. Naunyn-Schmiedeberg's Archives of Pharmacology, 360, 5–13.

Podar K, & Anderson KC (2008). The pathophysiologic role of VEGF in hematologic malignancies. Clinical Research, 105(4), 1383–1395. 10.1182/blood-2004-07-2909

Pyne NJ, & Pyne S (2011). Receptor tyrosine kinase-G-protein-coupled receptor signalling platforms: Out of the shadow? Trends in Pharmacological Sciences, 32(8), 443–450. 10.1016/j.tips.2011.04.002 [PubMed: 21612832]

Ren J, Wang Q, Morgan S, Si Y, Ravichander A, Dou C, … Liu B (2014). Protein kinase C-δ (PKCδ) regulates proinflammatory chemokine expression through cytosolic interaction with the NF-κB subunit p65 in vascular smooth muscle cells. Journal of Biological Chemistry, 289(13), 9013–9026. 10.1074/jbc.M113.515957 [PubMed: 24519937]

Rhee SG (2001). Regulation of phosphoinositide-specific phospholipase C. Annual Review of Biochemistry, 70, 281–312. 10.1146/annurev.physiol.65.092101.142517

Sivaraj KK, Li R, Albarran-Juarez J, Wang S, Tischner D, Grimm M, … Wettschureck N (2015). Endothelial Gα q/11 is required for VEGF- induced vascular permeability and angiogenesis. Cardiovascular Research, 108(1), 171–180. 10.1093/cvr/cvv216 [PubMed: 26272756]

Syrovatkina V, Alegre KO, Dey R, & Huang XY (2016). Regulation, signaling, and physiological functions of G-proteins. Journal of Molecular Biology, 428(19), 3850–3868. 10.1016/j.jmb.2016.08.002 [PubMed: 27515397]

Turner N, & Grose R (2010). Fibroblast growth factor signalling: From development to cancer. Nature Reviews Cancer, 10(2), 116–129. 10.1038/nrc2780 [PubMed: 20094046]

Wang K, Song Y, Chen D-B, & Zheng J (2008). Protein phosphatase 3 differentially modulates vascular endothelial growth factor- and fibroblast growth factor 2-stimulated cell proliferation and signaling in ovine fetoplacental artery endothelial cells. Biology of Reproduction, 79(4), 704–710. 10.1095/biolreprod.108.068957 [PubMed: 18509162]

Wang K, & Zheng J (2012). Signaling regulation of fetoplacental angiogenesis. Journal of Endocrinology, 212(3), 243–255. 10.1530/JOE-11-0296 [PubMed: 22106098]

Wettschureck N, & Offermanns S (2005). Mammalian G proteins and their cell type specific functions. Physiological Review, 85(4), 1159–1204. 10.1152/physrev.00003.2005

Xia C, Bao Z, Yue C, Sanborn BM, & Liu M (2001). Phosphorylation and regulation of G-protein-activated phospholipase C-β3 by cGMP-dependent protein kinases. Journal of Biological Chemistry, 276(23), 19770–19777. 10.1074/jbc.M006266200 [PubMed: 11278298]

Yue C, Dodge KL, Weber G, & Sanborn BM (1998). Phosphorylation of serine 1105 by protein kinase A inhibits phospholipase Cbeta3 stimulation by Galphaq. Journal of Biological Chemistry, 273(29), 18023–18027. 10.1074/JBC.273.29.18023 [PubMed: 9660757]

Yue C, Ku C-Y, Liu M, Simon MI, & Sanborn BM (2000). Molecular mechanism of the inhibition of phospholipase C β3 by protein kinases. Journal of Biological Chemistry, 275(39), 30220–30225. 10.1074/jbc.M004276200 [PubMed: 10893237]

Yue C, & Sanborn BM (2001). KN-93 inhibition of G protein signaling is independent of the ability of Ca^{2+}/calmodulin-dependent protein kinase II to phosphorylate phospholipase Cβ3 on 537-Ser. Molecular and Cellular Endocrinology, 175(1–2), 149–156. 10.1016/S0303-7207(01)00383-5 [PubMed: 11325525]

Zamudio S (2007). High-altitude hypoxia and preeclampsia. Frontiers in Bioscience, 12, 2967–2977. [PubMed: 17485273]

Zeng H, Zhao D, & Mukhopadhyay D (2002). KDR stimulates endothelial cell migration through heterotrimeric G protein Gq/11-mediated activation of a small GTPase RhoA. Journal of Biological Chemistry, 277(48), 46791–46798. 10.1074/jbc.M206133200 [PubMed: 12244099]

Zeng H, Zhao D, Yang S, Datta K, & Mukhopadhyay D (2003). Heterotrimeric Gαq/Gα11 proteins function upstream of vascular endothelial growth factor (VEGF) receptor-2 (KDR) phosphorylation in vascular permeability factor/VEGF signaling. Journal of Biological Chemistry, 278(23), 20738–20745. 10.1074/jbc.M209712200 [PubMed: 12670961]

Zhao Y-J, Zou Q-Y, Li Y, Li H-H, Wu Y-M, Li X-F, … Zheng J (2014). Expression of G-protein subunit α−14 is increased in human placentas from preeclamptic pregnancies. The Journal of Histochemistry and Cytochemistry: Official Journal of the Histochemistry Society, 62(5), 347–354. 10.1369/0022155414521213 [PubMed: 24423937]

Zhou C, Zou Q-Y, Li H, Wang R-F, Liu A-X, Magness RR, & Zheng J (2017). Preeclampsia downregulates microRNAs in fetal endothelial cells: Roles of miR-29a/c-3p in endothelial function. The Journal of Clinical Endocrinology & Metabolism, 102(9), 3470–3479. 10.1210/jc.2017-00849 [PubMed: 28911139]

Zou Q, Zhao Y, Li H, Wang X, Liu A, Zhong X, … Zheng J (2018). GNA11 differentially mediates fibroblast growth factor 2- and vascular endothelial growth factor A-induced cellular responses in human fetoplacental endothelial cells. Journal of Physiology, 596(12), 2333–2344. 10.1113/JP275677 [PubMed: 29659033]

Zygmunt M, Herr F, Münstedt K, Lang U, & Liang OD (2003). Angiogenesis and vasculogenesis in pregnancy. European Journal of Obstetrics, Gynecology, and Reproductive Biology, 110(SUPPL), 10–18. 10.1016/S0301-2115(03)00168-4

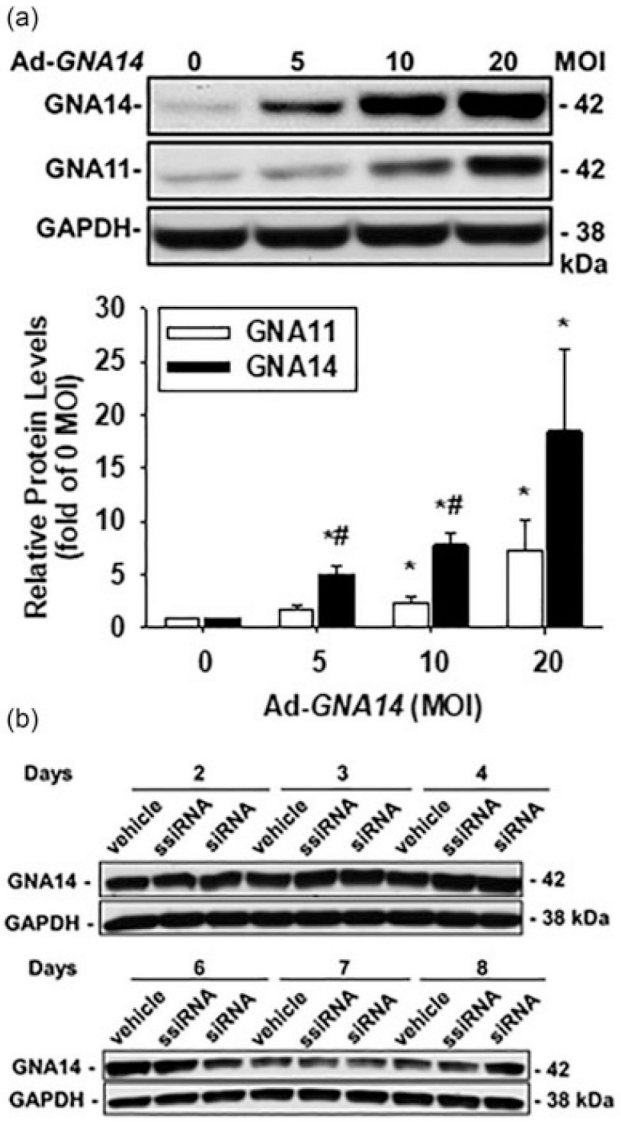

FIGURE 1.

Effects of Ad-*GNA14* and GNA14 siRNA on protein levels of GNA14 in HUVECs. (a) Ad-*GNA14* transfection: After 3 days of transfection, cellular proteins (20–30 μg) were subjected to Western blot analysis for GNA14, GNA11, and GAPDH. Data normalized to GAPDH were expressed as means ± SEM. *Means differ from 0 MOI control (SNK method for pairwise multiple comparisons); #means differ from GNA11 at the corresponding dose of Ad-*GNA14* (Student's *t*-test). $p < 0.05$; $n = 4$ individual experiments. (b) Western blot analysis images for GNA14 siRNA transfection: After transfecting with a single dosing of 20 nM of GNA14 siRNA for up to 4 days (upper panel) or with double dosing (Days 1 and 6) of 20 nM GNA14 siRNA for up to 8 days (lower panel), cells were harvested and cellular proteins (20–30 μg) were subjected to western blot analysis. $n = 4$ individual experiments. GNA, G protein α subunit; HUVECs, human umbilical cord endothelial cells; MOI, multiplicity of infection; siRNA, small interfering RNA; ssiRNA, scrambled siRNA

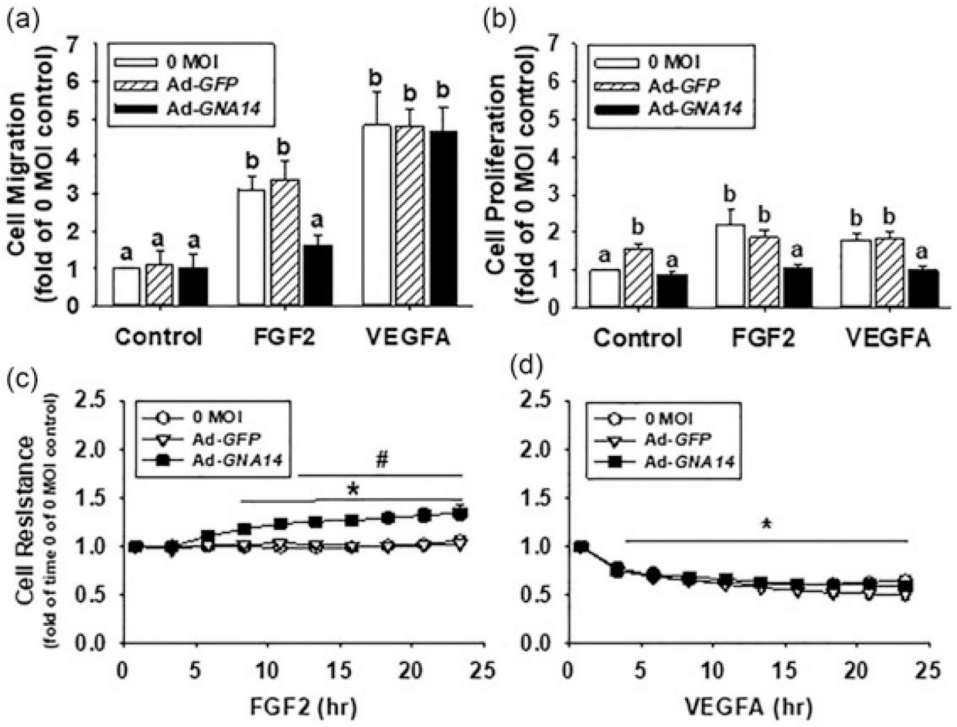

FIGURE 2.

Effects of Ad-*GNA14* on FGF2- and VEGFA-induced cell migration, proliferation, and monolayer integrity in HUVECs. Cell migration (a), proliferation (b), and permeability (c) were determined using Transwell system, CCK-8, and ECIS, respectively. Cells were transfected with Ad-*GFP* or Ad-*GNA14* at 5 MOI for 2 days. After serum starvation for additional 24 hr (cell migration and cell proliferation) or 3 hr (cell permeability), cells were treated with FGF2 and VEGFA (100 ng/ml) for 16 hr (cell migration; $n = 3–5$ individual experiments), 48 hr (cell proliferation; $n = 4$ individual experiments) or 24 hr (cell permeability; $n = 3$ individual experiments). Data were expressed as means ± SEM. [a,b]Means with different letters differ (SNK method for pairwise multiple comparisons). *Means differ from the time 0 control of 0 MOI (SNK method for pairwise multiple comparisons); [#]means differ from the corresponding dose of Ad-GFP (Student's *t*-test). $p < 0.05$. ECIS: electric cell–substrate impedance sensing system; FGF2: fibroblast growth factor 2; GNA: G protein α subunit; HUVECs: human umbilical cord endothelial cells; MOI: multiplicity of infection; SNK: Student-Newman–Keuls; VEGFA: vascular endothelial growth factor A

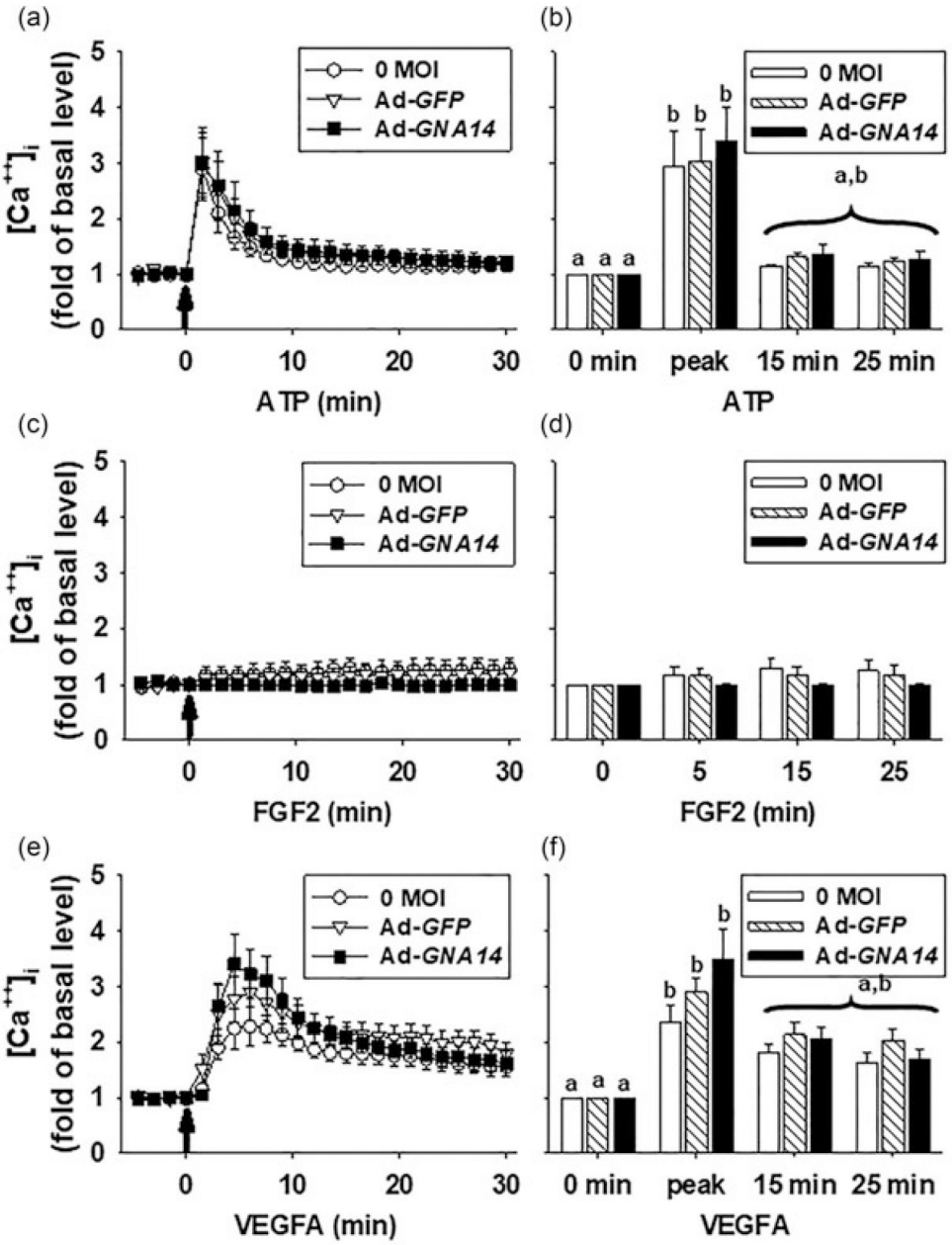

FIGURE 3.

Effects of Ad-*GNA14* on $[Ca^{++}]_i$ in response to ATP, FGF2, or VEGFA. Cells were transfected by Ad-*GFP* or Ad-*GNA14* at 5 MOI for 3 days. Cells were loaded with Fura-2 AM for 1 hr, and incubated in Krebs buffer for ester hydrolysis for 0.5 hr. 80–90 cells were randomly selected for real-time $[Ca^{++}]_i$ imaging under microscope. After basal levels of $[Ca^{++}]_i$ were recorded for 5 min, ATP, FGF2, or VEGFA was added, followed by sequentially recording $[Ca^{++}]_i$ for up to 24 hr. (a, c, and e): $[Ca^{++}]_i$ of responding cells (ATP and VEGFA) or of all cells selected (FGF2). (b, d, and f): $[Ca^{++}]_i$ at different time points. Data were expressed as means ± SEM fold of mean of the last min of basal levels. Arrow:

Addition of agonists. [a,b]Means with different letters differ (SNK method for pairwise multiple comparisons). $p < 0.05$. $n = 3–5$ individual experiments.

ATP: adenosine triphosphate; FGF2: fibroblast growth factor 2; GNA: G protein α subunit; MOI: multiplicity of infection; SNK:

Student-Newman–Keuls; VEGFA: vascular endothelial growth factor A

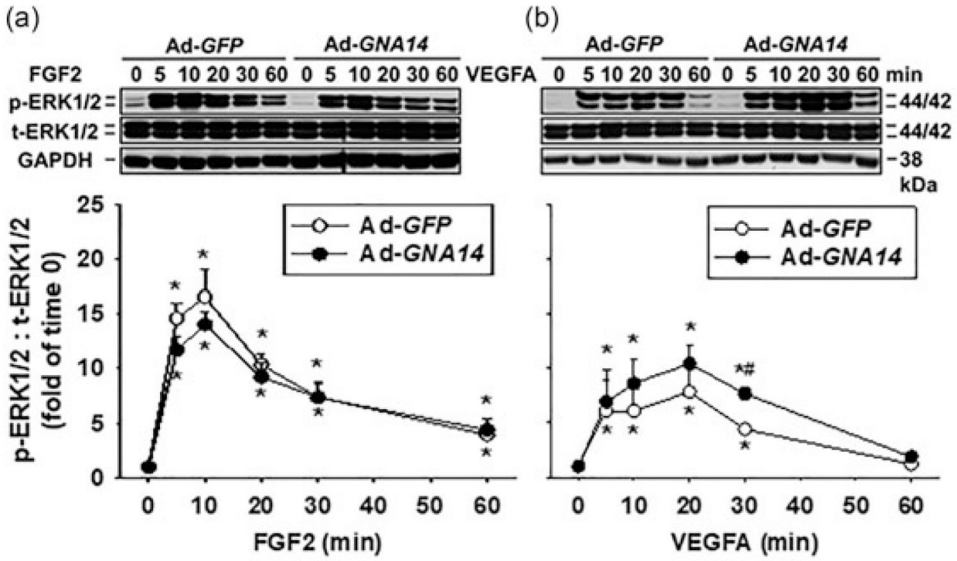

FIGURE 4.

Effects of Ad-*GNA14* on FGF2- and VEGFA-induced phosphorylation of ERK1/2. Cells were transfected with Ad-*GFP* or Ad- *GNA14* for 2 days. After serum starvation for additional 24 hr, cells were treated with FGF2 and VEGFA (100 ng/ml). Cellular proteins (20–30 μg) were subjected to western blot analysis. Data were expressed as means ± SEM. *Means differ from the corresponding time 0 (SNK method for pairwise multiple comparisons); #means differ from corresponding time point of the Ad-*GFP* group (Student's *t*-test). $p < 0.05$; $n = 4$ individual experiments. FGF2: fibroblast growth factor 2; GNA: G protein α subunit; SNK: Student-Newman–Keuls; VEGFA: vascular endothelial growth factor A

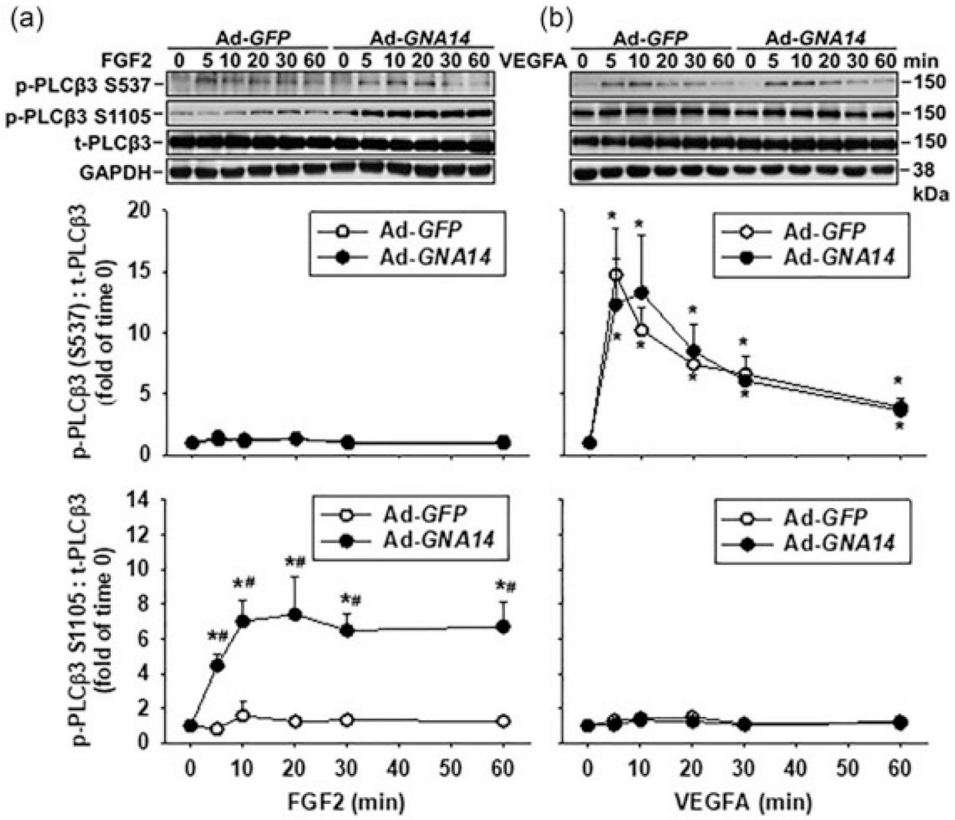

FIGURE 5.

Effects of Ad-*GNA14* on phosphorylation of PLC*β*3 S537 and S1105. After 2 days of transfection, HUVECs were serum starved for additional 24 hr. Cells were treated with FGF2 and VEGFA (100 ng/ml). Cellular proteins (20–30 μg) were subjected for western blot analysis. Data were expressed as means ± SEM. *Means differ from the corresponding time 0 (SNK method for pairwise multiple comparisons);

#different from the corresponding time point of Ad-*GFP* (Student's *t*-test); $p < 0.05$; $n = 3$ individual experiments. FGF2: fibroblast growth factor 2; GNA: G protein α subunit; SNK: Student-Newman–Keuls; VEGFA: vascular endothelial growth factor A

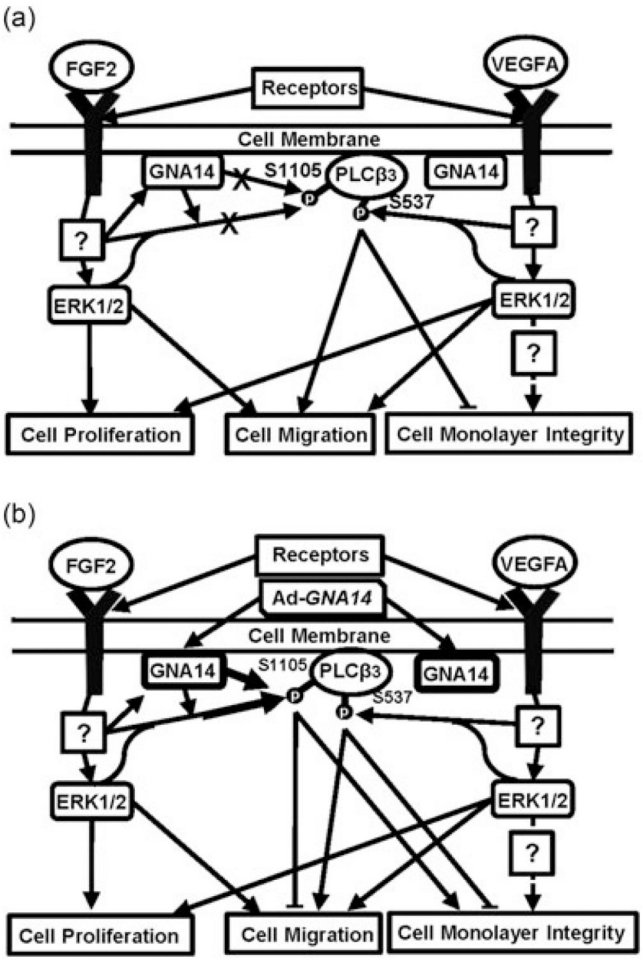

FIGURE 6.

A hypothesized signaling model for the role of GNA14 in FGF2- and VEGFA-regulated fetal endothelial function via PLCβ3 and ERK1/2 under physiological chronic low oxygen. (a) Ad*GFP* (a control): Under this condition, FGF2- and VEGFA stimulate cell proliferation and migration at least via activation of ERK1/2 (Jiang et al., 2013b). GNA14 at the basal level does not affect RTK downstream signals-mediated phosphorylation of PLCβ3 S537 and S1105 in response to FGF2. However, whereas VEGFA increases phosphorylation of PLCβ3 S537, but not S1105, in association with VEGFA-increased cell proliferation, migration, and permeability, GNA14 does not appear to mediate all these changes as GNA14 overexpression does not dysregulate all these cellular responses as shown in (b). (b) GNA14 overexpression by Ad-*GNA14*: Upon FGF2 stimulation, RTK downstream signals activate GNA14 (possibly via phosphorylation). This activated form of overexpressed GNA14 facilitates PLCβ3 S1105 phosphorylation in response to FGF2 by directly acting and/or indirectly via enhancing activity of RTK downstream signals on PLCβ3 S1105. Such excessive phosphorylation may inhibit FGF2-stimulated cell migration and enhance FGF2-maintained cell monolayer integrity. In contrast, GNA14 overexpression does not affect PLCβ3 S537 phosphorylation and cell function in response to VEGFA. Crosses: Blocked or no stimulation; bold-lined squares: Increased GNA14 protein; bold arrows: Enhanced

stimulation; question marks: Unknown signals. FGF2: fibroblast growth factor 2; GNA: G protein α subunit; RTK: receptor tyrosine kinase; VEGFA: vascular endothelial growth factor A

TABLE 1

Antibodies used in Western blot analysis

Antibody	Vendor	Catalog number	Dilution
GAPDH	Novus Biologicals (Littleton, CO)	H00002597-M01	1:10,000
GNA11	Abgent (Suzhou, China)	AP19441a	1:1,000
GNA14	Abnova (Taipei, Taiwan, China)	H00009630-M06A	1:500
Phospho-p44/42 MAPK T202/Y204 (p-ERK1/2)	Cell Signaling Technology (Denvers, MA)	9101	1:2,000
p44/42 MAPK (t-ERK1/2)	Cell Signaling Technology	9102	1:2,000
Phospho-PLCβ3 S537 (p-PLCβ3 S537)	Cell Signaling Technology	2481	1:500
Phospho-PLCβ3 S1105 (p-PLCβ3 S1105)	Thermo Fisher Scientific (Waltham, MA)	PA5–38089	1:1,000
PLCβ3 (t-PLCβ3)	Millipore (Billerica, MA)	ABS-512	1:1,000